Effect of Variability in Anatomical Landmark Location on Knee Kinematic Description

Nicholas A. Morton,[1] Lorin P. Maletsky,[1] Saikat Pal,[2] Peter J. Laz[2]

[1]Department of Mechanical Engineering, University of Kansas, 1530 W. 15th Street, Learned Hall, Room 3138, Lawrence, Kansas 66045

[2]Department of Mechanical and Materials Engineering, University of Denver, 2390 South York Street, Denver, Colorado 80208

Received 21 November 2005; accepted 11 January 2007

Published online in Wiley InterScience (www.interscience.wiley.com). DOI 10.1002/jor.20396

ABSTRACT: Small variability associated with identifying and locating anatomical landmarks on the knee has the potential to affect the joint coordinate systems and reported kinematic descriptions. The objectives of this study were to develop an approach to quantify the effect of landmark location variability on both tibiofemoral and patellofemoral kinematics and to identify the critical landmarks and associated degrees of freedom that most affected the kinematic measures. The commonly used three-cylindric open-chain kinematic description utilized measured rigid body kinematics from a cadaveric specimen during simulated gait. A probabilistic analysis was performed with 11 anatomical landmarks to predict the variability in each kinematic. The model predicted the absolute kinematic bounds and offset kinematic bounds, emphasizing profile shape, for each kinematic over the gait cycle, as well as the range of motion. Standard deviations of up to 2 mm were assumed for the anatomical landmark locations and resulted in significant variability in clinically relevant absolute kinematic parameters of up to 6.5° and 4.4 mm for tibiofemoral and 7.6° and 6.5 mm for patellofemoral kinematics. The location of the femoral epicondylar prominences had the greatest effect on both the tibiofemoral and patellofemoral kinematic descriptions. A quantitative understanding of the potential changes in kinematic description caused by anatomical landmark variability is important not only to the accuracy of kinematic gait studies and the evaluation of total knee arthroplasty implant performance, but also may impact component placement decision-making in computer-assisted surgery. © 2007 Orthopaedic Research Society. Published by Wiley Periodicals, Inc. J Orthop Res

Keywords: knee kinematics; anatomical landmarks; probabilistic methods; kinematic variability

INTRODUCTION

Knee kinematics are required in a wide range of biomechanics areas to characterize gait, to diagnose knee pathologies, and to evaluate total knee arthroplasty (TKA) designs and outcomes.[1–7] Kinematics are measured and described using a variety of techniques, with the most common method to describe the relative motion of joint coordinate systems (JCS) that are attached to the bones.[8] While different ways exist for locating the JCS,[9–12] researcher identified anatomical landmarks are typical,[13–16] specifically when describing kinematics using a three-cylindric open-chain model.[17–19] The kinematic description of Grood and Suntay[17] defines the flexion–extension (F–E) axis as fixed to the femur, the internal–external (I–E) axis as fixed to the tibia, and a varus–valgus (V–V) axis as able to "float" between the two axes in such a way that it is always perpendicular to the other axes.[8,17] The relative motion (translations and rotations) between the tibia and femur are then described using these axes. Although less agreement exists on describing patellar motion relative to the femur, a common method is to determine the rotations using a three-cylindric open chain model as in the tibiofemoral description, while describing the patellofemoral translations relative to the JCS fixed to the femur.[19]

The landmarks used to define the JCS can be identified using different methods. For live subjects, easily palpable bony features are often identified using a probe with various measurement systems. Coordinate systems can also be defined using images such as those obtained from magnetic resonance technology[20–22] or fluoroscopy.[23,24] A fixed helical axis[9,12,25] can be used to eliminate the variability in probing anatomical landmarks, although the accurate identification of the helical

Correspondence to: Lorin P. Maletsky (Telephone: 785-864-2985; Fax: 785-864-5152; E-mail: maletsky@ku.edu)

axis in a cadaveric specimen can be problematic. The accuracy of identifying landmarks that are used to create the JCS has been examined, with significant variability reported for inter-observer and intra-observer identification.[20,22,26]

While the effects of variability in the landmarks on knee kinematics has been characterized in several studies,[20,26] a combined tibiofemoral and patellofemoral evaluation using probabilistic methods and accounting for variable interaction effects has not been previously performed, to our knowledge. Probabilistic modeling provides an ideal platform for evaluating the effect of variability in landmark identification on kinematics. While probabilistic modeling has been applied to the structural reliability of orthopedic implants,[27–29] little research has applied the techniques to evaluate the variability in kinematics.[30] In the probabilistic analysis, the locations of the landmarks were modeled as distributions and a more comprehensive envelope of results for each kinematic degree of freedom was predicted. The probabilistic approach accounts for potential variable interaction effects as a priori knowledge of the combination of landmark uncertainty values resulting in extreme positions is not always possible. In addition, the most important parameters affecting each kinematic are identified through sensitivity factors. Thus, the objectives of this study were to develop an approach to quantify how variability in the location of the anatomical landmarks affects the described tibiofemoral and patellofemoral kinematics using probabilistic techniques and to identify the critical landmarks affecting the absolute and offset kinematics.

METHODS

Rigid body motion of the femur, tibia, and patella were measured for a cadaver in a knee simulator.[31] Anatomical landmarks were probed using an Optotrak 3020 optical system with a rigid-body probe (Northern Digital Inc., Waterloo, Ontario, Canada) to define the JCS, which were used to convert the rigid body motion to the reported tibiofemoral and patellofemoral kinematics. Eleven landmarks were used to define the three JCSs fixed to the femur, tibia, and patella (Fig. 1).

The femoral coordinate system was defined by three landmarks: the lateral and medial epicondylar prominences and the geometric center of the proximal femur, which was cut approximately 18 cm above the joint line. The medial–lateral (M–L) axis of the femur was defined by the transepicondylar line, positive to the right independent

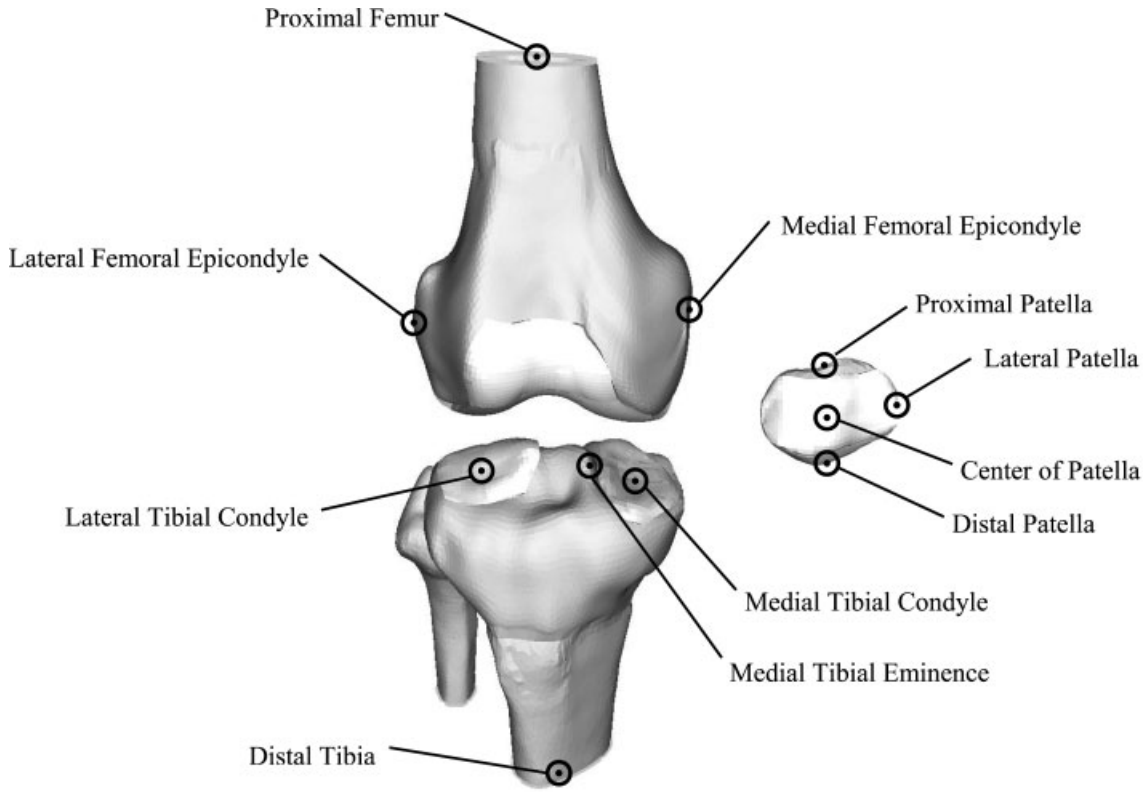

Figure 1. Schematic of 11 anatomical landmarks used to define fixed-body coordinate systems on the femur, tibia, and patella.

 DOI 10.1002/jor

of right or left leg, with the origin of the coordinate system defined as the midpoint. By convention, this axis is directed left to right for proper construction of a right-handed coordinate system. The anteroposterior (A–P) axis was formed by taking the cross-product of the M–L axis and the line from the origin to the center of the proximal femur with anterior positive. The superior–inferior (S–I) axis was then defined as the cross-product of the M–L and A–P axes yielding a superiorly directed axis. This method for creating the femoral coordinate system is similar to that described by Pennock and Clark[18] with the exception of identifying the proximal femur as the center of the cut bone as opposed to the hip center, because the latter was unavailable on the dissected cadaveric specimen.

The tibial reference frame, constructed using the method described by Grood and Suntay,[17] was defined using the centers of the lateral and medial condyles, the proximal tip of the medial spine of the tibial eminence, and the center of the distal tibia, which was cut approximately 18 cm below the joint line. The origin of the system, based on the Pennock and Clark JCS,[18] was located at the proximal tip of the medial eminence, and the S–I axis was defined from the center of the distal tibia to the origin. The A–P axis was defined as the cross-product of the S–I axis and the line connecting the centers of the tibial condyles. The M–L axis was determined by the cross-product of the A–P and S–I axes.

Lastly, the patellar reference frame was defined using four landmarks identified on the posterior, articular surface: the proximal, distal, and lateral points around the articular periphery, and the center of the patella.[19] The proximal, distal, and center were located using the patellar ridge with the origin of the patellar coordinate system identified roughly as the geometric center. These retropatellar points were visible following parapatellar incision and lateral reflection of the patella and quadriceps tendon. To orient the patellar coordinate system, the vector connecting the proximal and distal patellar landmarks defined the S–I axis. The A–P axis was defined by the cross-product of the S–I axis and the vector connecting the lateral patellar prominence with the center of the proximal and distal patellar landmarks. The M–L axis was then defined by the cross-product of the S–I and A–P axes.

The rotations and translations of the tibia relative to the femur were described using a three-cylindric open chain.[8,17] The patellofemoral rotations were described in a similar way to the tibiofemoral rotations, while the translations were expressed as the motion of the patellar origin relative to the anatomical reference frame fixed to the femur.[19,32]

Each of the 11 anatomical landmarks was represented by normal distributions in three orthogonal degrees of freedom (M–L, A–P, and S–I). A single surgeon probed the landmarks that were used as the mean positions, while standard deviations for each of the directions were estimated based on limited experimental data collected within the laboratory on two different knees with multiple researchers (Table 1). These internal studies used human cadaver knees to identify the same

Table 1. Standard Deviations of Anatomical Landmark Locations (mm)

	della Croce et al.[a]			Internal Study Number 1[b]			Internal Study Number 2[c]			Probabilistic Study		
Landmark	M–L	A–P	S–I	M–L	A–P	S–I	M–L	A–P	S–I	M–L	A–P	S–I
Lateral femoral epicondyle	7.8	3.9	4.9	2.2	7.0	7.8	0.7	0.8	3.4	2.0	2.0	2.0
Medial femoral epicondyle	6.7	5.1	5.0	1.7	0.8	4.0	—	—	—	2.0	2.0	2.0
Proximal femur	—	—	—	0.7	0.7	2.0	0.4	0.8	2.5	1.0	1.0	2.0
Lateral tibial condyle	5.6	8.0	2.1	2.0	2.2	1.3	1.9	1.4	0.7	1.0	1.0	0.5
Medial tibial condyle	6.6	3.4	4.4	2.4	2.4	0.4	—	—	—	1.0	1.0	0.5
Medial tibial eminence	6.6	2.2	2.6	1.4	4.7	2.7	—	—	—	1.0	1.0	0.5
Distal tibia	—	—	—	0.5	0.5	0.9	0.1	0.7	1.0	1.0	1.0	2.0
Proximal patella	—	—	—	2.2	1.8	0.5	1.0	0.8	0.9	1.0	1.0	1.0
Distal patella	—	—	—	3.2	1.4	2.6	0.7	1.0	1.1	1.0	1.0	1.0
Lateral patella	—	—	—	2.1	1.0	1.2	1.4	0.5	1.0	1.0	1.0	1.0
Retropatellar center	—	—	—	2.9	0.3	1.5	2.4	0.4	2.5	2.0	1.0	2.0

[a]della Croce et al. collected by physical therapists via external palpation ($n = 6$).[26]
[b]Internal study #1 by three orthopedic surgeons and two research professionals via disarticulated cadaver knee ($n = 5$).
[c]Internal study #2 by graduate research assistants via disarticulated cadaver knee ($n = 7$).

set of anatomical points using similar measurement equipment and represent data that were most similar to what was used for the knee examined in this study. Data for similar landmarks from a study palpating landmarks on live subjects[26] are also shown in Table 1 for comparison. The accuracy in identifying the landmarks is highly dependent on equipment used, technique, and researcher. The values used in this study reflect the difficulty in identifying certain features that are not clearly visible, such as the epicondylar landmarks, compared to estimating the center of a visible geometry such as the center of the tibial condyles.

The motions of the femur, tibia, and patella were measured with a cadaveric knee using a dynamic force-controlled knee simulator.[31,33] The knee simulator is an electro-hydraulic system that uses actuators to impart a vertical force and flexion angle at the hip, a quadriceps load, and an adduction–abduction force, tibial torque, and F–E moment at the ankle. An Optotrak system recorded the motion of rigid body markers attached to each of the bones during the gait cycle. The result was a series of time-dependent transformation matrices that defined the relative motion of the rigid bodies over the gait cycle. Probed anatomical landmarks were measured relative to the appropriate rigid bodies and used to locate and orient the JCS. A single profile of measured rigid body motion was utilized in this study, with variability in landmark location affecting the definition of the JCS and thus the described joint kinematics.

The probabilistic analysis was performed by combining Nessus® (SwRI, San Antonio, TX) with the kinematic description presented. A Monte Carlo simulation and Advanced Mean Value (AMV) method, described in Haldar and Mahadevan,[34] were used to perform the probabilistic analysis. Results from the more efficient AMV method were compared to the results from a 1,000-trial Monte Carlo simulation to confirm convergence. Kinematics are commonly described using absolute or offset values. Absolute values are presented relative to the specific coordinate system identified for that specific knee and are used to show the "true" knee position. Offset values are used to accentuate the motion occurring during an activity and are found by translating the curve during a gait cycle so that it starts at the initial baseline position at 0% of the cycle. For each kinematic degree of freedom, the probabilistic model predicted the 1, 50, and 99 percentile results. The 50 percentile or baseline results represented the deterministic prediction, corresponding to each landmark located at its mean position. The 1% and 99% absolute and offset bounds were also determined. Range of motion (ROM), referring to the differences between the maximum and minimum position during a gait cycle, was determined for the 1%, 50%, and 99% offset kinematics.

Reported sensitivity factors were relative measures of how each kinematic measure was affected by variability in each landmark, as well as each direction. Sensitivities were calculated with the AMV method based on the unit vector specifying the most probable point in the transformed standard normal variate space.[34] As a result, the sum of the squares of the sensitivity factors for all of the variables was unity. The sensitivity of each kinematic metric to each landmark degree of freedom was computed at every 1.33% of the gait cycle (77 computations/cycle). To provide a ranking of importance, the absolute value of the sensitivity factors were averaged over the gait cycle.

RESULTS

The probabilistic model predicted absolute and offset bounds of the kinematics for six tibiofemoral degrees of freedom (Fig. 2: F–E, V–V, and I–E rotations; and M–L, A–P, and S–I translations) and six patellofemoral degrees of freedom (Fig. 3: F–E, M–L, and I–E tilt rotations; M–L shift, A–P run, and S–I glide translations). Heel strike occurred at 0% gait with toe-off at ~65% gait. Normally offset kinematics start at zero, but were shown as starting at the baseline absolute values at heel strike for clarity. The 1% and 99% lines represent the kinematic bounds for the profiles at each time-step and are not representative of a single gait profile. The magnitudes of the absolute and offset bounds are presented as the average difference between the bounds and the baseline over the gait cycle (Table 2). The offset kinematics exhibited larger differences between the baseline and the bounds during swing phase than during stance phase; however, the absolute kinematics displayed similar differences between the upper and lower absolute bounds in stance and swing phase, with the shape of the absolute bounds being similar to the baseline shape for most kinematic measures.

ROM serves as an indicator of the variability in the offset kinematics between different specimens or testing conditions. Observing the difference in offset ROM results for a kinematic measure relates the extent to which the shape of the kinematic measure changes with variability in probed landmarks. For tibiofemoral A–P position, a mean ROM of 2.2 mm was predicted with bounds (1%–99%) ranging from 2.1 to 4.6 mm, even though the actual motion was identical. For I–E rotation, the mean ROM was 5.4° with bounds ranging from 3.8° to 7.1° (Table 2). For some kinematics, ROM was greater for bounds in both directions as seen in the 1% and 99% offset kinematics, for example, tibiofemoral V–V (Table 2 and Fig. 2b).

The sensitivity factors reported are the absolute values of the sensitivities averaged over the gait cycle and show the effects of the variability of the anatomical landmarks on the six tibiofemoral kinematics (Fig. 4) and six patellofemoral kinematics (Fig. 5). Sensitivities are reported by row for

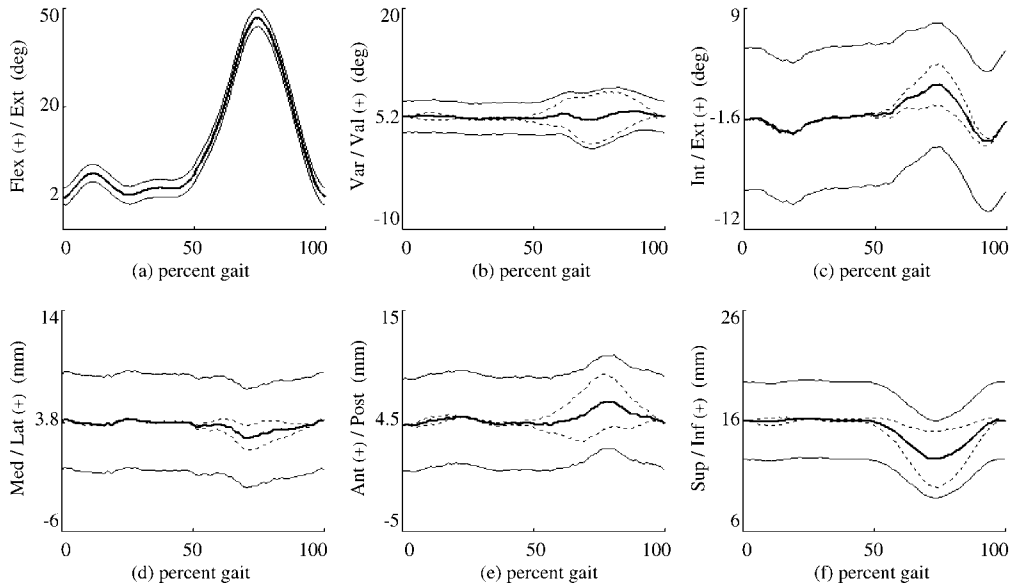

Figure 2. Absolute and offset bounds (1 to 99%) for kinematic descriptions of tibiofemoral (a) F–E, (b) V–V, and (c) I–E rotations; and (d) M–L, (e) A–P, and (f) S–I translations for a gait cycle. Absolute and offset bounds depicted by thin solid lines and broken lines, respectively. Baseline gait reported with thick solid line.

each kinematic measure and by column for each direction of the landmark variability. For example, for tibiofemo A–P kinematics, the kinematics were most sensitive to the S–I and A–P position of the epicondyles, while the absolute kinematics were most impacted by the A–P and S–I position of the epicondyles and the tibial medial eminence. The two femoral epicondylar landmarks consistently had the largest overall effects on the tibiofemoral kinematics (Fig. 4), with the A–P degree of freedom having the highest sensitivity for both the offset and absolute description of kinematics. The tibial landmarks affected absolute kinematics but generally minimally affected the offset kinematics. Tibiofemoral ROM was predominantly affected by the epicondylar points. The patellofemoral sensitivity data (Fig. 5) also exhibited a large dependence on the epicondylar points. The three points around the periphery of the patella affected the patellar rotations, mainly in the absolute kinematic description, but had no effect on the patellar translation. Conversely, the geometric center of the patella significantly affected the patellar translations, with no sensitivity on patellar rotations.

DISCUSSION

A quantitative understanding of the potential variability present in reported kinematics is important to biomechanical gait and simulator studies. By utilizing a probabilistic approach to consider the variability of identifying all of the anatomic landmarks simultaneously, we provided a comprehensive representation of experimental practice. The absolute and offset bounds and ROMs conveyed additional information that can provide insight into the joint kinematics. A large envelope for the absolute kinematic description means that the apparent absolute position of the knee had changed relative to the origin, which may be predominantly caused by the origin moving. The offset kinematic descriptions emphasize changes in profile shape and provide a good method for comparing and evaluating kinematic data from multiple knees or comparing data between labs, since these measures are less sensitive to landmark variability. The ROMs provide an indication of the overall relative motion or sliding distance that has the potential to impact wear in TKA patients.

Kinematic measures with large ROM were not particularly susceptible to differences caused by variability in locating anatomical coordinate frames. For most motions, there were considerable changes in magnitude between the baseline and either bound for ROM (Table 2). This variability can be seen by examining the ROM for the two offset bounding curves. In the cases of tibiofemoral V–V (Fig. 2b) and patellofemoral I–E tilt (Fig. 3c), the small ROM of the baseline curve (50%) and the large differences during swing phase in the 1% and

Table 2. Probabilistic Model Results: Absolute Baseline Position, Average Differences between 1%–50% and 50%–99% Bounds for Absolute and Offset Kinematics, and the Range of Motion Results for each Kinematic Measure

	TF Rotation (degrees)			TF Translation (mm)			PF Rotation (degrees)			PF Translation (mm)		
Variable	F–E	V–V	I–E	M–L	A–P	S–I	F–E	Rotation	Tilt	Shift	Run	Glide
Baseline position	2.1	5.2	−1.6	3.8	4.5	16.0	11.9	3.7	−13.6	5.3	35.3	23.5
Average absolute differences	2.2	2.5	6.5	4.4	4.2	3.5	6.0	7.3	7.6	6.5	4.1	5.7
Average offset differences	0.2	2.1	1.0	0.7	1.6	1.5	0.2	1.1	1.1	1.5	1.2	0.7
1% offset ROM	45.2	3.7	3.8	2.9	2.1	6.1	25.8	1.1	3.3	3.8	8.6	30.2
50% offset ROM	45.5	1.2	5.4	1.8	2.2	3.7	26.0	2.7	1.8	1.7	6.8	28.9
99% offset ROM	45.7	3.7	7.1	0.7	4.6	1.3	26.2	4.5	2.9	1.7	5.4	27.7

99% envelopes of the offset kinematics caused the ROM for both the upper and lower bounds to be larger than the baseline (Table 2). Conclusions based upon small improvements to the kinematic results should be scrutinized, as subject differences may be an artifact of kinematic description uncertainty, rather than component performance.

The small variability in landmark position resulted in significant envelopes in multiple clinically relevant kinematic measures. Studies have documented significant changes in tibiofemoral implant wear with varying levels and combinations of A–P position and I–E rotation.[1,3,35] The predicted bounds (1%–99%) were 2.5 mm for A–P position and 3.3° for I–E rotation, representing 113% and 61% of the mean value. In comparisons between standard (A–P: 0–10 mm; I–E: ±5°) and reduced (A–P: 0–5 mm; I–E: ±2.5°) kinematic levels, McEwen et al. quantified a fourfold reduction in wear rate.[35] Although the magnitudes observed from the landmark variability in our study were smaller, the large percent differences in these kinematic measures can lead to potentially significant differences in experimental wear simulators and component performance. The A–P translation is highly dependent on the S–I and A–P locations of the epicondylar axis; great care should be taken to correctly and consistently identify these points in the sagittal plane if A–P motion is of interest. The potential use of a tibiofemoral screw axis may help minimize this variability. Care must be exercised when utilizing measured subject kinematics for simulator testing or implant evaluation, as well as when applying laboratory findings to the patient-specific clinical environment.

Similarly, the apparent variability observed in V–V may have implications on condylar liftoff especially since varus or valgus motion may have occurred based on the offset bounds (Fig. 2b). The greatest variability in V–V occurred during the swing phase at high flexion angles, which is also the region when condylar liftoff is most commonly observed in fluoroscopy studies.[23,36] Trying to predict condylar liftoff based on V–V data for the knee examined in this study, or even which side lifted off, would be questionable. The shapes of the V–V curves are highly dependent on the location of the epicondylar landmarks, specifically in the A–P direction.

Patellar maltracking, often cited as a common cause of TKA revision surgery, is most influenced by I–E tilt and M–L shift.[2,4,7,37] Although the variability in ROM was relatively small for these two motions, ranging from 1.8° to 3.3° for I–E tilt

DOI 10.1002/jor

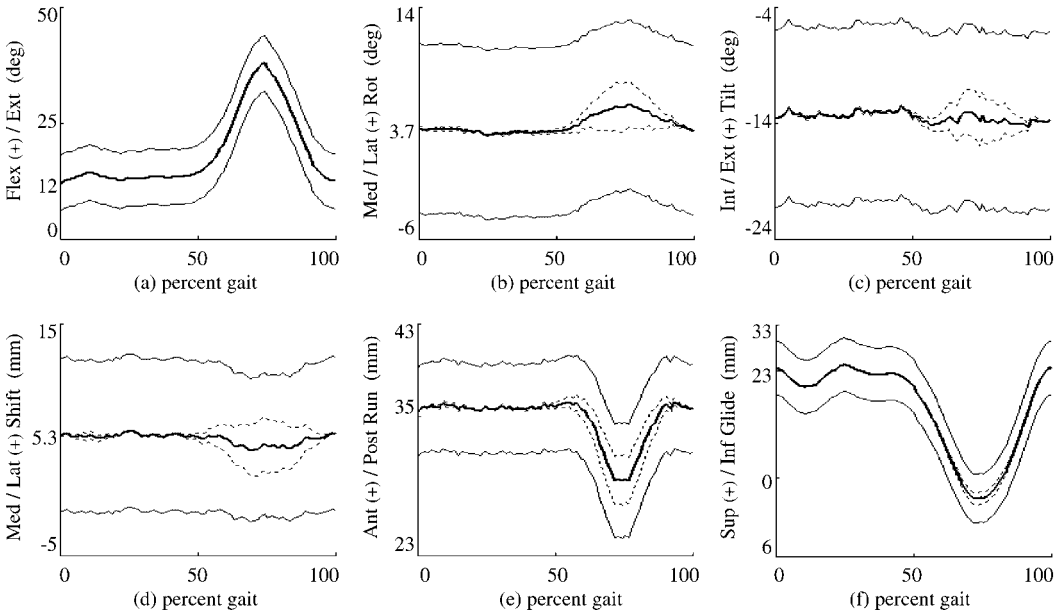

Figure 3. Absolute and offset bounds (1–99%) for kinematic descriptions of patellofemoral (a) F–E, (b) M–L, and (c) I–E tilt rotations; and (d) M–L shift, (e) A–P run, and (f) S–I glide translation for a gait cycle. Absolute and offset bounds depicted by thin solid lines and broken lines, respectively. Baseline gait reported with thick solid line.

Sensitivities		
○	None	S = 0.0
⊙	Low	S < 0.23
◡	↓	S < 0.46
◎		S < 0.7
●	High	S > 0.7

		Femoral Anatomical Landmarks									Tibial Anatomical Landmarks											
		L Epicondyle			M Epicondyle			Proximal			Lateral			Medial			M Eminance			Distal		
		ML	AP	SI	ML	AP	SI	ML	AP	SI	ML	AP	SI	ML	AP	SI	ML	AP	SI	ML	AP	SI
F-E	Offset Kinematics	◡	◎	⊙	◡	◎	⊙	◡	⊙	⊙	○	○	○	○	○	○	◡	⊙	⊙	◡	⊙	⊙
	Absolute Kinematics	⊙	●	⊙	⊙	◡	⊙	⊙	◎	⊙	○	○	○	○	○	○	⊙	◎	⊙	⊙	◎	⊙
V-V	Offset Kinematics	⊙	●	⊙	⊙	●	⊙	⊙	⊙	⊙	○	○	○	○	○	○	⊙	⊙	○	⊙	⊙	⊙
	Absolute Kinematics	◎	◡	⊙	◎	◡	⊙	◎	⊙	⊙	○	○	○	○	○	○	◎	⊙	⊙	◎	⊙	⊙
I-E	Offset Kinematics	◎	◡	⊙	◎	◡	⊙	◎	⊙	◡	○	⊙	○	○	⊙	○	⊙	⊙	○	⊙	⊙	⊙
	Absolute Kinematics	⊙	◎	⊙	⊙	◎	⊙	⊙	⊙	⊙	○	●	○	○	●	○	⊙	⊙	○	⊙	⊙	⊙
M-L	Offset Kinematics	⊙	●	⊙	⊙	●	⊙	⊙	⊙	⊙	○	○	○	○	○	○	⊙	◡	⊙	○	○	○
	Absolute Kinematics	●	⊙	⊙	●	⊙	⊙	⊙	⊙	⊙	○	○	○	○	○	○	●	⊙	⊙	○	○	○
A-P	Offset Kinematics	⊙	◡	●	⊙	◡	●	⊙	⊙	⊙	○	○	○	○	○	○	⊙	⊙	⊙	⊙	⊙	⊙
	Absolute Kinematics	⊙	●	◡	⊙	◎	◡	⊙	⊙	⊙	○	○	○	○	○	○	⊙	●	⊙	⊙	⊙	⊙
S-I	Offset Kinematics	⊙	●	⊙	⊙	●	⊙	○	○	○	○	○	○	○	○	○	⊙	⊙	⊙	⊙	⊙	⊙
	Absolute Kinematics	⊙	◡	●	⊙	◡	●	○	○	○	○	○	○	○	○	○	⊙	⊙	◡	⊙	⊙	⊙

Figure 4. Sensitivity (S) of tibiofemoral kinematic description to anatomical landmark location.

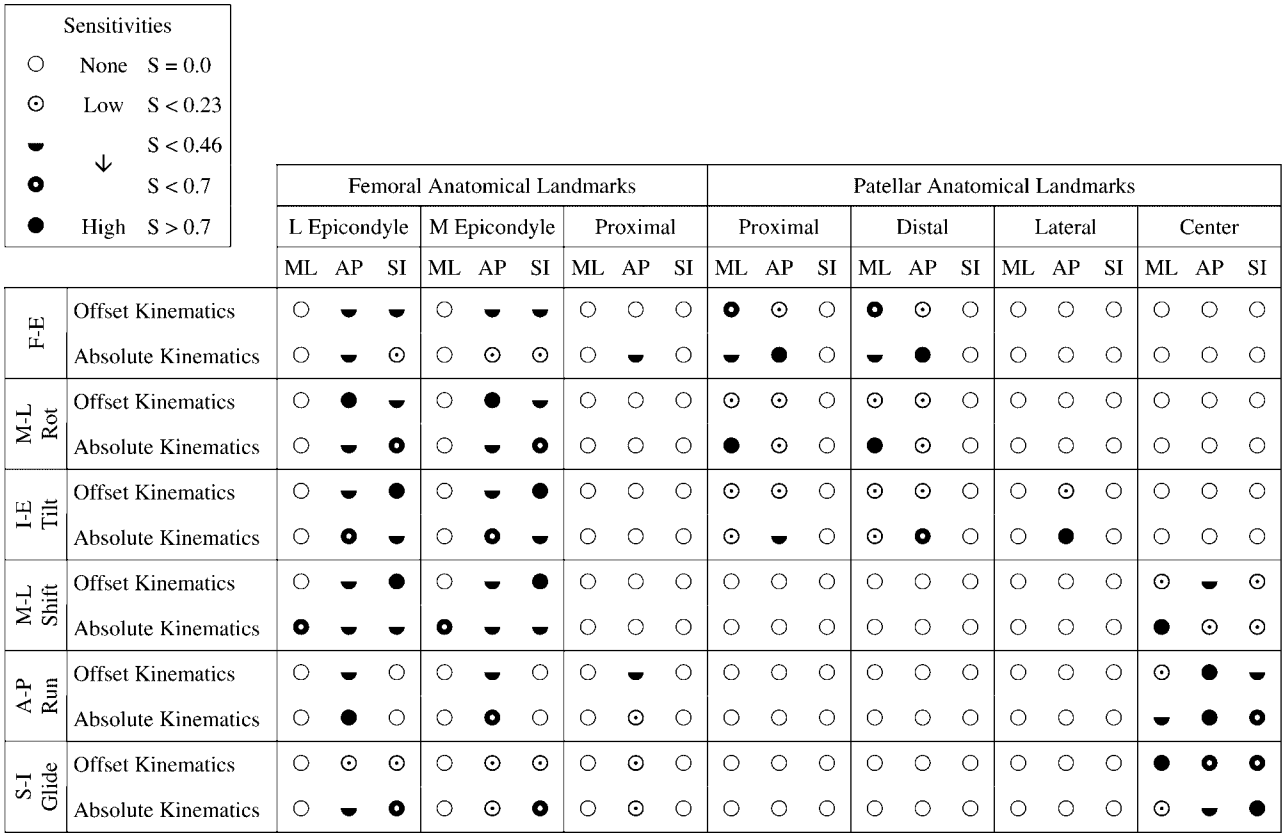

Figure 5. Sensitivity (S) of patellofemoral kinematic description to anatomical landmark location.

and from 1.7 mm to 3.8 mm for M–L shift (Table 2), large variability was observed in the envelope of absolute position for I–E tilt and M–L shift with average differences of $\pm 7.6^{\circ}$ and ± 6.5 mm, respectively. Although not affecting the actual contact pressure distribution and wear, researchers should understand the effects of landmark location variability when interpreting patellofemoral kinematics.

The findings of this study are based on the rigid body motions and landmark locations from a single cadaver. The results are relatively independent of the methods used to measure the rigid body motion and landmark locations, although the methods would affect the accuracy of the rigid body motions and the landmark positions. The method of defining the JCS from the landmarks greatly affects the reported kinematic description and the sensitivities. As reported in the literature[25,26,38–40] and affirmed in this study, kinematic results were most sensitive to variability in locating the femoral epicondylar landmarks. The JCS used for this study relied on identifying the epicondylar axis to define the F–E axis,[18] but other systems define the F–E axis on the femur differently. The common Grood and Suntay system uses two posterior points on the distal condyles[17] and Della Croce suggested using a series of landmarks to define the F–E axis.[41] Our results suggest that the F–E axis definition is the most critical in all of the systems. One advantage of using posterior landmarks on the distal femur is that the A–P variation should be smaller, which would improve the data since A–P variability was shown to be a sensitive variable for most of the kinematics.

The proximal femur and distal tibial landmarks had little effect on the offset kinematic descriptions. The medial and lateral tibial condylar landmarks were significant to the absolute description of tibiofemoral I–E rotation and had little effect on the offset kinematic descriptions and ROM. The peripheral patella landmarks were used to create the rotational alignment of the patella coordinate frame and, therefore, these points had no effect on the translational kinematic measures. Likewise, the geometric center of the patella, defining the origin of the patellar coordinate system, affected the translations, but not the rotational kinematic measures.

The magnitude of the kinematic envelopes and the reported sensitivity factors are dependent on

 DOI 10.1002/jor

the standard deviation levels of the anatomical landmark locations assumed, although similar sensitivities would be expected for different standard deviation levels if their relative values remained the same. The largest standard deviation assumed was 2.0 mm, which is considerably smaller than the standard deviations determined by della Croce[26] on patient data collected by six physical therapists via external palpation. Additionally, the standard deviations for the epicondylar landmarks were the same in all directions showing the relative sensitivity of the directional variability, without biasing a particular direction. The A–P direction of the epicondylar landmarks was consistently more significant than the other degrees of freedom.

In conclusion, the effects of landmark location variability on kinematic descriptions were quantified and the critical landmarks affecting kinematics identified. The probabilistic approach provided the ability to account for landmark location variability in reported kinematic studies, the understanding of which has implications on the testing and analyses used to evaluate implant performance. In addition, the epicondylar landmarks were determined to be the most critical landmark affecting offset kinematics for both tibiofemoral and patellofemoral kinematics; however, when the absolute description of kinematics is of interest (e.g., potential impingement, implant edge loading), the variability in the other landmarks should also be considered. While the current study focused on kinematic description, the variability in landmark location may similarly affect the emerging field of computer-assisted surgery (CAS) where landmarks are defined by probing points and surfaces, or extracting locations from images, with the potential variability associated with landmark location influencing component placement.

ACKNOWLEDGMENTS

This study was supported in part by DePuy, a Johnson & Johnson Company.

REFERENCES

1. Blunn GW, Walker PS, Joshi A, et al. 1991. The dominance of cyclic sliding in producing wear in total knee replacements. Clin Orthop Relat Res 273:253–260.
2. Katchburian MV, Bull AM, Shih YF, et al. 2003. Measurement of patellar tracking: assessment and analysis of the literature. Clin Orthop Relat Res 412:241–259.
3. Kawanabe K, Clarke IC, Tamura J, et al. 2001. Effects of A–P translation and rotation on the wear of UHMWPE in a total knee joint simulator. J Biomed Mater Res 54:400–406.
4. Kawano T, Miura H, Nagamine R, et al. 2002. Factors affecting patellar tracking after total knee arthroplasty. J Arthroplasty 17:942–947.
5. Walker PS, Haider H. 2003. Characterizing the motion of total knee replacements in laboratory tests. Clin Orthop Relat Res 410:54–68.
6. Walker PS, Sathasivam S., 2000. Design forms of total knee replacement. Proc Inst Mech Eng [H] 214:101–119.
7. Yoshii I, Whiteside LA, Anouchi YS. 1992. The effect of patellar button placement and femoral component design on patellar tracking in total knee arthroplasty. Clin Orthop Relat Res 275:211–219.
8. Wu G, Cavanagh PR. 1995. ISB recommendations for standardization in the reporting of kinematic data. J Biomech 28:1257–1261.
9. Mannel H, Marin F, Claes L, et al. 2004. Establishment of a knee-joint coordinate system from helical axes analysis—a kinematic approach without anatomical referencing. IEEE Trans Biomed Eng 51:1341–1347.
10. Ramsey DK, Wretenberg PF. 1999. Biomechanics of the knee: methodological considerations in the in vivo kinematic analysis of the tibiofemoral and patellofemoral joint. Clin Biomech (Bristol, Avon) 14:595–611.
11. Cheze L. 2000. Comparison of different calculations of three-dimensional joint kinematics from video-based system data. J Biomech 33:1695–1699.
12. Woltring HJ, Huiskes R, de Lange A, et al. 1985. Finite centroid and helical axis estimation from noisy landmark measurements in the study of human joint kinematics. J Biomech 18:379–389.
13. Koh TJ, Grabiner MD, De Swart RJ. 1992. In vivo tracking of the human patella. J Biomech 25:637–643.
14. Lafortune MA, Cavanagh PR, Sommer HJ III, et al. 1992. Three-dimensional kinematics of the human knee during walking. J Biomech 25:347–357.
15. van Kampen A, Huiskes R. 1990. The three-dimensional tracking pattern of the human patella. J Orthop Res 8:372–382.
16. Bull AM, Amis AA. 1998. Knee joint motion: description and measurement. Proc Inst Mech Eng [H] 212:357–372.
17. Grood ES, Suntay WJ. 1983. A joint coordinate system for the clinical description of three-dimensional motions: application to the knee. J Biomech Eng 105:136–144.
18. Pennock GR, Clark KJ. 1990. An anatomy-based coordinate system for the description of the kinematic displacements in the human knee. J Biomech 23:1209–1218.
19. Bull AM, Katchburian MV, Shih YF, et al. 2002. Standardisation of the description of patellofemoral motion and comparison between different techniques. Knee Surg Sports Traumatol Arthrosc 10:184–193.
20. Lerner AL, Tamez-Pena JG, Houck JR, et al. 2003. The use of sequential MR image sets for determining tibiofemoral motion: reliability of coordinate systems and accuracy of motion tracking algorithm. J Biomech Eng 125:246–253.
21. von Eisenhart-Rothe R, Siebert M, Bringmann C, et al. 2004. A new in vivo technique for determination of 3D kinematics and contact areas of the patello-femoral and tibio-femoral joint. J Biomech 37:927–934.
22. Fellows RA, Hill NA, Macintyre NJ, et al. 2005. Repeatability of a novel technique for in vivo measurement of three-dimensional patellar tracking using magnetic resonance imaging. J Magn Reson Imaging 22:145–153.

23. Dennis D, Komistek R, Scuderi G, et al. 2001. In vivo three-dimensional determination of kinematics for subjects with a normal knee or a unicompartmental or total knee replacement. J Bone Joint Surg [Am] 83-A (Suppl 2 Pt 2):104–115.
24. Li G, Wuerz TH, DeFrate LE. 2004. Feasibility of using orthogonal fluoroscopic images to measure in vivo joint kinematics. J Biomech Eng 126:314–318.
25. Besier TF, Sturnieks DL, Alderson JA, et al. 2003. Repeatability of gait data using a functional hip joint centre and a mean helical knee axis. J Biomech 36:1159–1168.
26. della Croce U, Cappozzo A, Kerrigan DC. 1999. Pelvis and lower limb anatomical landmark calibration precision and its propagation to bone geometry and joint angles. Med Biol Eng Comput 37:155–161.
27. Browne M, Langley RS, Gregson PJ. 1999. Reliability theory for load bearing biomedical implants. Biomaterials 20:1285–1292.
28. Dar FH, Meakin JR, Aspden RM., 2002. Statistical methods in finite element analysis. J Biomech 35:1155–1161.
29. Nicolella DP, Thacker BH, Katoozian H, et al. 2006. The effect of three-dimensional shape optimization on the probabilistic response of a cemented femoral hip prosthesis. J Biomech 39:1265–1278.
30. Laz PJ, Pal S, Halloran JP, et al. 2006. Probabilistic finite element prediction of knee wear simulator mechanics. J Biomech 39:2303–2310.
31. Maletsky LP, Hillberry BM., 2005. Simulating dynamic activities using a five-axis knee simulator. J Biomech Eng 127:123–133.
32. Hefzy MS, Jackson WT, Saddemi SR, et al. 1992. Effects of tibial rotations on patellar tracking and patello-femoral contact areas. J Biomed Eng 14:329–343.
33. Guess TM, Maletsky LP. 2005. Computational modelling of a total knee prosthetic loaded in a dynamic knee simulator. Med Eng Phys 27:357–367.
34. Haldar A, Mahadevan S. 2000. Probability, reliability, and statistical methods in engineering design. New York/Chichester, UK: John Wiley & Sons.
35. McEwen HM, Barnett PI, Bell CJ, et al. 2005. The influence of design, materials and kinematics on the in vitro wear of total knee replacements. J Biomech 38:357–365.
36. Dennis DA, Komistek RD, Walker SA, et al. 2001. Femoral condylar lift-off in vivo in total knee arthroplasty. J Bone Joint Surg [Br] 83:33–39.
37. Stiehl JB, Komistek RD, Dennis DA, et al. 2001. Kinematics of the patellofemoral joint in total knee arthroplasty. J Arthroplasty 16:706–714.
38. Piazza SJ, Cavanagh PR. 2000. Measurement of the screw-home motion of the knee is sensitive to errors in axis alignment. J Biomech 33:1029–1034.
39. Blankevoort L, Huiskes R, de Lange A. 1988. The envelope of passive knee joint motion. J Biomech 21:705–720.
40. Most E, Axe J, Rubash H, et al. 2004. Sensitivity of the knee joint kinematics calculation to selection of flexion axes. J Biomech 37:1743–1748.
41. Della Croce U, Camomilla V, Leardini A, et al. 2003. Femoral anatomical frame: assessment of various definitions. Med Eng Phys 25:425–431.

 DOI 10.1002/jor